

## **ELECTRONIC BEAM STEERING USING SWITCHED PARASITIC SMART ANTENNA ARRAYS**

**P. K. Varlamos and C. N. Capsalis**

National Technical University of Athens  
Department of Electrical and Computer Engineering  
Division of Information Transmission Systems  
and Material Technology  
9, Iroon Polytechniou Str., Athens 15773, Greece

**Abstract**—A method of designing smart antennas based on switched parasitic antenna arrays is presented in this paper. The direction of maximum gain can be controlled by a digital word, while the selection of element spacing and weighting is optimized using the method of genetic algorithms. Various results are presented to show how antennas of this type perform, outlining the advantages and limitations of their design.

### **1 Introduction**

### **2 Genetic Algorithms for Antenna Design**

### **3 Switched Parasitic Antenna Arrays: Basic Theory**

### **4 Numerical Results**

### **5 Conclusions**

### **References**

## **1. INTRODUCTION**

Electronic beam steering can be used in mobile applications to enhance spectrum efficiency as well as reduce the problems associated with multipath propagation. Switched parasitic smart antenna arrays have the ability to adjust their radiation pattern in a way that their main beam always points at the direction of the mobile receiver or transmitter. Simply inserting an appropriate digital word in the antenna's feeding circuit can do this. The 1's and the 0's in the

digital word represent the active and parasitic elements in the array, respectively. There are  $2^N - 1$  possible combinations of 1's and 0's ( $N$ -number of elements) with each one of them giving a radiation pattern with its own characteristics. Because of the symmetry of each radiation pattern, the design of the antenna aims at the coverage of the azimuth plane above the  $x$ -axis, meaning offering directions of maximum gain every  $20^\circ$  between  $0^\circ$  and  $180^\circ$ . Each one of the main beams may be produced simply selecting the combination of active and parasitic elements, which results in the desired radiation pattern. The well-known genetic algorithms may carry out the evaluation of the element spacing and weighting, which optimize the antenna performance.

Genetic algorithms (GA's) are a class of search techniques that use the mechanics of natural selection and genetics (crossover, mutation) to conduct a global search of a solution space [1]. Other optimization techniques (such as gradient descent methods) are suitable for problems that have a small number of parameters and, hence, a small solution space, because of their ability to search a region of the solution space around the initial guess for the best local solution. However, as the number of parameters and the size of the solution space increase, gradient methods often get stuck at poor solutions, if the initial guess falls in a region full of poor solutions [2]. A typical multi-parameter problem is the design and synthesis of antennas, where a set of performance criteria, such as gain, maximum sidelobe level and beamwidth, should be met. The difficulty of providing a good initial guess makes other optimization methods inappropriate and underlines the need for the ability that GA's exhibit to conduct a global search of the solution space [3].

This paper presents a method of electronic beam steering using switched parasitic antenna arrays. Various efforts have been made in the past to use both active and parasitic elements to achieve electronic beam steering [4–6]. The interesting part of this method is the insertion of a digital word to control the antenna radiation pattern and the optimization of the antenna design using GA's.

## 2. GENETIC ALGORITHMS FOR ANTENNA DESIGN

Genetic algorithms search the solution space of a function through the use of simulated evolution. In general, the fittest individuals of any population tend to reproduce and survive to the next generation. However, inferior individuals can, by chance, survive and also reproduce. Genetic algorithms have the ability to explore all regions of the state space through selection, crossover and mutation operations applied to individuals in the population [7].

The selection of individuals plays an important role in a genetic algorithm. A probabilistic selection is performed based on the individual's fitness, in a way that the better chromosomes have an increased chance of being selected. Roulette wheel is the type of selection considered here. The probability  $P_i$  for each individual is defined by

$$P_i = \frac{f_i}{\sum_{j=1}^{PopSize} f_j} \quad (1)$$

where

$$\begin{array}{ll} f_i & \text{the fitness of individual } i \\ \sum_{j=1}^{PopSize} f_j & \text{the average population fitness} \end{array}$$

Elitism is also taken into account with at least one copy of the best individual of the population being passed to the next generation [7].

Genetic operators provide the basic search mechanism in the GA. Crossover takes two individuals and produces two new individuals while mutation alters one individual to produce a new solution. For binary chromosomes, simple crossover and binary mutation are considered [7]. Simple crossover generates a random number  $r$  from a uniform distribution from 1 to  $m$  (chromosome length) and creates two new individuals according to the following equations:

$$x'_i = \begin{cases} x_i, & i < r \\ y_i, & \text{otherwise} \end{cases} \quad (2)$$

$$y'_i = \begin{cases} y_i, & i < r \\ x_i, & \text{otherwise} \end{cases} \quad (3)$$

Binary mutation flips each bit in every individual in the population with probability  $p_m$  according to equation (4)

$$x'_i = \begin{cases} 1 - x_i, & U(0, 1) < p_m \\ x_i, & \text{otherwise} \end{cases} \quad (4)$$

The objective function is the driving force behind the GA. It is called from the GA to determine the fitness of each solution string generated during the search. The objective function here is the number of different directions of maximum gain every  $20^\circ$  between  $0^\circ$  and  $180^\circ$  (i.e.,  $10^\circ, 30^\circ, 50^\circ, 70^\circ, 90^\circ, 110^\circ, 130^\circ, 150^\circ, 170^\circ$ ) among the  $2^N - 1$  radiation patterns. Directions of maximum gain which appear more

than once do not change the value of the objective function, but are all available so that the designer selects the best of them, after the design of the antenna. For instance the fitness of an individual (i.e., element spacing and weighting) that gives at least one direction of maximum gain at  $10^\circ$ ,  $50^\circ$ ,  $90^\circ$ ,  $130^\circ$  and  $170^\circ$  of the azimuth plane is equal to 5. The goal is to find an individual with fitness equal to 9, which offers beamwidths of at least  $20^\circ$  and relative sidelobe levels not more than  $-3$  dB.

### 3. SWITCHED PARASITIC ANTENNA ARRAYS: BASIC THEORY

The mathematical model for the antenna factor of an array of  $N$  dipoles is given by [8]

$$AF(\theta, \phi) = \sum_{m=1}^N w_m c_m e^{jkr_m \cos \psi_m} \quad (5)$$

where

$$\begin{aligned} c_m &= \frac{I_m}{I_1} && \text{the relative excitation coefficients} \\ &I_1 && \text{the excitation of element 1} \\ k &= \frac{2\pi}{\lambda} && \\ &\lambda && \text{wavelength} \\ r_m, \psi_m &&& \text{as shown in Fig. 1} \\ w_m &= e^{j\delta_m} && \text{array weight at element } m \end{aligned}$$

As for  $\cos \psi_m$ , it is given by

$$\cos \psi_m = \cos \theta_m \cos \theta + \sin \theta_m \sin \theta \cos(\phi - \phi_m) \quad (6)$$

where

$$\theta_m, \phi_m \quad \text{the elevation and azimuth angle of element } m$$

The antenna factor of a linear array lying along the  $x$ -axis, which has been used in the subsequent calculations, can be expressed as

$$AF(\theta, \phi) = \sum_{m=1}^N w_m c_m e^{jkd_m \cos \psi_m} \quad (7)$$

where

$$d_m \quad \text{as shown in Fig. 2}$$

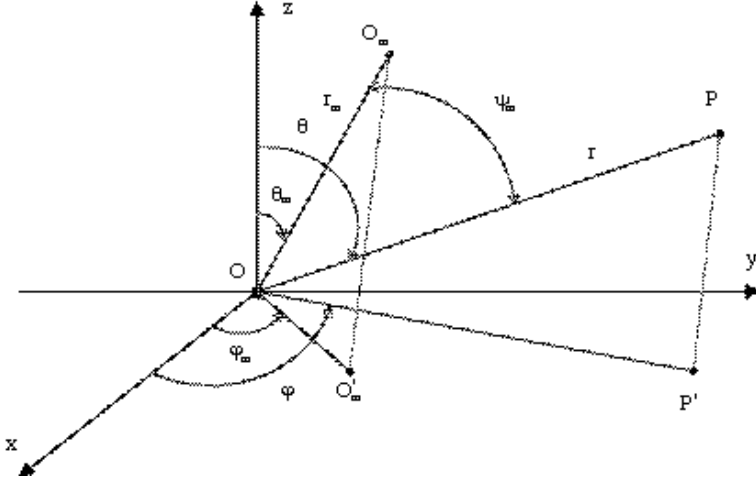


**Figure 1.** Geometry of an array.

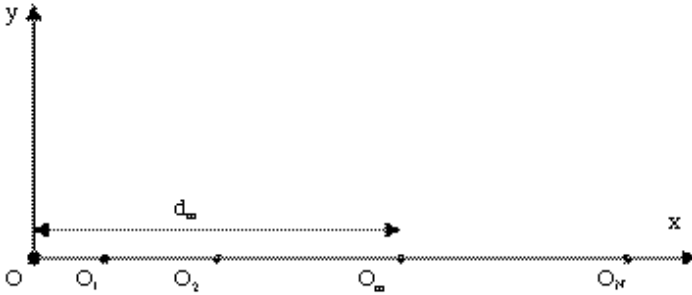


**Figure 2.** Geometry of a linear array lying along the  $x$ -axis.

As for  $\cos \psi_m$ , it is given by (6) for  $\theta_m = 90^\circ$ ,  $\phi_m = 0^\circ$

$$\cos \psi_m = \sin \theta \cos \phi \quad (8)$$

The antenna factor for the  $x$ - $y$  plane ( $\theta = 90^\circ$ ) is given by

$$AF(\phi) = \sum_{m=1}^N w_m c_m e^{jkd_m \cos \phi} \quad (9)$$

The radiation pattern for the azimuth plane can be expressed as

$$U(\phi) = U_0(\theta = 90^\circ, \phi) \cdot |AF(\phi)|^2 \quad (10)$$

where

$U_0(\theta, \phi)$  the radiation pattern of a single element

If each element is a dipole of length  $L$ ,  $U_0$  is given by

$$U_0(\theta) = A \left( \frac{\cos \left( k \frac{L}{2} \cos \theta \right) - \cos \left( k \frac{L}{2} \right)}{\sin \theta} \right)^2, \quad A \text{ constant} \quad (11)$$

The excitations  $I_m$  ( $m = 1, \dots, N$ ) at the input terminals (mutual coupling induces the input currents of the parasitic elements) are related to the terminal voltages of the elements by the impedance matrix  $Z$ :

$$V = Z \cdot I \quad (12a)$$

where

$$\begin{aligned} V &= [V_1 \ \dots \ V_n]^{-1}, \quad I = [I_1 \ \dots \ I_N]^{-1} \\ \text{and} \quad Z &= \begin{bmatrix} Z_{11} & Z_{12} & \dots & Z_{1N} \\ Z_{21} & Z_{22} & \dots & Z_{2N} \\ \vdots & \vdots & & \vdots \\ Z_{N1} & Z_{N2} & \dots & Z_{NN} \end{bmatrix} \end{aligned}$$

The terminal voltages of the active elements can be taken equal to each other and those of the parasitic elements are equal to zero, so the digital word inserted in the antenna's feeding circuit is the normalized voltage vector.

Through (12a), the terminal voltage of any one element can be expressed in terms of the currents flowing in the others:

$$V_n = \sum_{m=1}^N Z_{nm} I_m \quad n = 1, \dots, N \quad (12b)$$

where  $Z_{nm}$  represents the mutual impedance between elements  $n, m$  ( $n \neq m$ ) or the self impedance of element  $m$  ( $n = m$ ).

The self impedance (referred to at the input current  $I_i$ ) of a dipole of length  $L$ , is given by [8]

$$Z_i = -\frac{1}{I_i^2} \int_{-L/2}^{L/2} E_z(\rho = a, z) I(z) dz \quad (13)$$

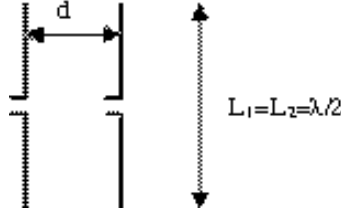


**Figure 3.** Configuration of two parallel dipoles at a distance  $d$ .

where

$$I(z) = I_m \sin \left[ k \left( \frac{L}{2} - |z| \right) \right] \quad (14)$$

the current distribution

$E_z$  the tangential electric field along the surface of the dipole and  
 $a$  the dipole radius

The mutual impedance (referred to at the input current  $I_{1i}$  of dipole 1) between two parallel dipoles at a distance  $d$  as shown in Fig. 3, is given by [8]

$$Z_{21i} = \frac{V_{21}}{I_{1i}} = -\frac{1}{I_{1i}I_{2i}} \int_{-L_2/2}^{L_2/2} E_{z21}(z)I_2(z)dz \quad (15)$$

where

$V_{21}$  the voltage induced in dipole 2 because of the current flowing in dipole 1  
 $E_{z21}$   $E$ -field component along the surface of dipole 2 radiated by dipole1, which is parallel to dipole 2  
 $I_2$  current distribution along dipole 2

The equations (13) and (15) can be solved and give the self and mutual impedance as functions of the ratios  $\frac{L}{\lambda}$ ,  $\frac{a}{\lambda}$  and  $\frac{L_1}{\lambda}$ ,  $\frac{L_2}{\lambda}$ ,  $\frac{d}{\lambda}$ , respectively [8].

#### 4. NUMERICAL RESULTS

The objective of the present design has been the coverage of the azimuth plane above the  $x$ -axis, offering directions of maximum gain every  $20^\circ$  between  $0^\circ$  and  $180^\circ$ . As an example, a switched parasitic smart antenna linear array of 10 dipoles was used, each one of them having length equal to  $\frac{\lambda}{2}$  and radius  $a = 0.001\lambda$ . To determine the

element spacing and weighting of the array, a GA was run until an individual with fitness equal to 9 was found. To be more precise, for each individual, the  $2^{10} - 1 = 1023$  radiation patterns available were checked (one for every combination of 1's and 0's in the digital word). The requirement was that at least 9 of them should have their main beams pointed at all possible directions every  $20^\circ$  between  $0^\circ$  and  $180^\circ$  (i.e., one combination having its main beam pointed at  $10^\circ$ , another at  $30^\circ$ , etc.). In addition, beamwidths of at least  $20^\circ$  and relative sidelobe levels not more than  $-3$  dB were expected. The GA evaluated the element spacing and weighting which fulfilled the requirements of the design. Table 1 shows the element spacing and phases  $\delta_m$  ( $w_m = e^{j\delta_m}$  the array weight at element  $m$ ). Table 2 shows the 9 digital words (each one of them representing a different direction of maximum gain), that were selected from a total of 46 digital words available. The reason for their selection was that they gave the best possible combinations of narrow beamwidths and low relative sidelobe levels. As one may see in Table 2, the directions of maximum gain were allowed to have a maximum deviation of  $\pm 2^\circ$  from the desired direction (e.g.,  $8.205^\circ$  instead of  $10^\circ$ , etc.). It is also obvious that the beamwidths proved to be much wider than expected, with their values varying from  $16^\circ$  to  $98^\circ$  (mean value at  $51.7^\circ$ ). As for the R.S.L's, they achieved satisfying values (even less than  $-7$  dB), and their mean value was calculated at  $-4.7$  dB.

**Table 1.** Element spacing and phases for the 10-element array.

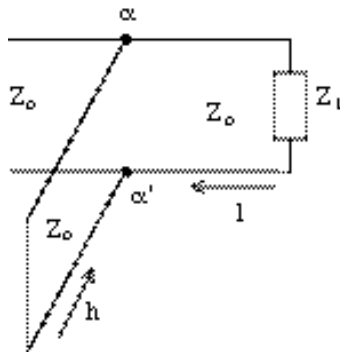
Element	Spacing ( $\lambda$ )	Phase (rad)
1	-	5.19316
2	0.07229	4.09086
3	0.67683	1.12838
4	0.11872	2.26443
5	0.41774	1.83410
6	0.13079	0.02608
7	0.14008	3.56847
8	0.06022	4.69302
9	0.38341	0.44414
10	0.52500	1.09956

A very important parameter of a switched parasitic antenna array is the evaluation of the input impedance to each active element of the



**Table 2.** Directions of maximum gain, beamwidths and relative sidelobe levels.

$n$	$V$	$\varphi_{max}(^\circ)$	$\varphi_{-}(^\circ)$	$\varphi_{+}(^\circ)$	$\Delta\varphi_{3dB}(^\circ)$	R.S.L. (dB)
953	1110111001	8.205	-34.78	34.78	69.56	-4.30
154	0010011010	28.864	-49.32	49.32	98.64	-3.46
772	1100000100	48.736	33.08	62.30	29.22	-3.54
634	1001111010	68.992	55.81	80.17	24.36	-4.72
76	0001001100	88.694	69.04	108.66	39.62	-7.34
307	0100110011	111.161	103.10	119.85	16.75	-3.94
606	1001011110	130.349	118.89	144.87	25.98	-6.36
446	0110111110	149.761	135.49	224.51	89.02	-3.98
284	0100011100	169.049	144.13	215.87	71.74	-4.74

**Figure 4.** Stub impedance matching configuration.

array. The input impedance of an active element is given by

$$Z_m^{in} = \frac{V_m}{I_m} \quad (16)$$

where

$$\begin{aligned} V_m & \text{ the normalized terminal voltage} \\ I_m & \text{ the current flowing in element } m \end{aligned}$$

The results of these calculations, for all the digital words in Table 2, are shown in Tables 3–5.

To achieve impedance matching at each element of the array, the well-known stub configuration, shown in Fig. 4, was used.  $Z_L$

**Table 3.** Input Impedance (I).

V	1110111001	0010011010	1100000100
$Z_{1,in}$	$154.81 + j86.82$	-	$153.22 + j61.88$
$Z_{2,in}$	$71.14 + j40.74$	-	$109.82 + j73.80$
$Z_{3,in}$	$20.06 + j43.90$	$24.78 + j59.31$	-
$Z_{4,in}$	-	-	-
$Z_{5,in}$	$132.84 - j19.77$	-	-
$Z_{6,in}$	$159.41 - j173.40$	$19.95 + j119.43$	-
$Z_{7,in}$	$3.51 + j49.08$	$3.12 + j48.55$	-
$Z_{8,in}$	-	-	$6.32 + j43.99$
$Z_{9,in}$	-	$77.80 + j31.58$	-
$Z_{10,in}$	$74.50 + j26.49$	-	-

**Table 4.** Input Impedance (II).

V	1001111010	0001001100	0100110011
$Z_{1,in}$	$13.20 + j46.02$	-	-
$Z_{2,in}$	-	-	$13.60 + j45.45$
$Z_{3,in}$	-	-	-
$Z_{4,in}$	$67.30 + j49.87$	$29.60 + j78.97$	-
$Z_{5,in}$	$78.72 - j31.24$	-	$150.17 - j51.08$
$Z_{6,in}$	$256.33 - j105.59$	-	$41.93 + j124.09$
$Z_{7,in}$	$4.15 + j46.43$	$20.88 + j115.66$	-
$Z_{8,in}$	-	$270.05 - j11.03$	-
$Z_{9,in}$	$81.93 + j33.06$	-	$62.84 + j17.49$
$Z_{10,in}$	-	-	$55.31 + j13.80$

represents the input impedance and  $Z_0$  was taken equal to  $50\Omega$ . For example, the first element of the array is active in four different voltage vectors. This means that the feeding line of the element should be connected through four on/off switches to four stubs. Depending on the digital word inserted in the antenna's feeding circuit, one stub should be "on" and the three others should be "off". The same procedure should be followed for all the elements. The results, meaning the values of  $l$  and  $h$  (see Fig. 4) for each stub, are shown in Tables 6–8.

**Table 5.** Input Impedance (III).

$V$	1001011110	0110111110	0100011100
$Z_{1,in}$	$12.52 + j46.78$	-	-
$Z_{2,in}$	-	$13.80 + j35.50$	$12.28 + j42.04$
$Z_{3,in}$	-	$22.20 + j42.24$	-
$Z_{4,in}$	$31.52 + j75.48$	-	-
$Z_{5,in}$	-	$159.52 - j1.08$	-
$Z_{6,in}$	$30.61 + j97.93$	$198.32 - j102.04$	$40.38 + j115.47$
$Z_{7,in}$	$339.20 - j166.51$	$271.56 - j110.69$	$236.15 - j212.13$
$Z_{8,in}$	$109.74 - j54.37$	$113.38 - j35.26$	$187.71 + j17.56$
$Z_{9,in}$	$72.97 + j2.06$	$75.22 + j4.69$	-
$Z_{10,in}$	-	-	-

**Table 6.** Parameters  $l, h$  for the stub impedance matching configuration (I).

$V$		1110111001		0010011010		1100000100	
$l_1(\lambda)$	$h_1(\lambda)$	0.20054	0.09133	-	-	0.19238	0.10008
$l_2(\lambda)$	$h_2(\lambda)$	0.21533	0.14561	-	-	0.20673	0.10543
$l_3(\lambda)$	$h_3(\lambda)$	0.30864	0.08553	0.28762	0.07956	-	-
$l_4(\lambda)$	$h_4(\lambda)$	-	-	-	-	-	-
$l_5(\lambda)$	$h_5(\lambda)$	0.15324	0.12150	-	-	-	-
$l_6(\lambda)$	$h_6(\lambda)$	0.16781	0.06536	0.27407	0.03995	-	-
$l_7(\lambda)$	$h_7(\lambda)$	0.34653	0.03082	0.34897	0.02913	-	-
$l_8(\lambda)$	$h_8(\lambda)$	-	-	-	-	0.34300	0.04446
$l_9(\lambda)$	$h_9(\lambda)$	-	-	0.19917	0.15556	-	-
$l_{10}(\lambda)$	$h_{10}(\lambda)$	0.19680	0.16502	-	-	-	-

The initial target of the present design was to cover the  $x$ - $y$  plane above the  $x$ -axis with 9 radiation patterns. The radiation pattern of a linear array of 10 dipoles of lengths equal to  $\frac{\lambda}{2}$ , taking into account (10) and (11), is given by

$$U(\phi) = A \cdot |AF(\phi)|^2, \quad A \text{ constant} \quad (17)$$

The polar diagrams of  $(U(\phi), \phi)$ , for the combinations of active and

**Table 7.** Parameters  $l, h$  for the stub impedance matching configuration (II).

$V$		1001111010		0001001100		0100110011	
$l_1(\lambda)$	$h_1(\lambda)$	0.32153	0.06542	-	-	-	-
$l_2(\lambda)$	$h_2(\lambda)$	-	-	-	-	0.32123	0.06701
$l_3(\lambda)$	$h_3(\lambda)$	-	-	-	-	-	-
$l_4(\lambda)$	$h_4(\lambda)$	0.22542	0.13250	0.27276	0.07014	-	-
$l_5(\lambda)$	$h_5(\lambda)$	0.10406	0.15534	-	-	0.15316	0.10450
$l_6(\lambda)$	$h_6(\lambda)$	0.17720	0.07231	-	-	0.25539	0.05616
$l_7(\lambda)$	$h_7(\lambda)$	0.34753	0.03456	0.27387	0.04210	-	-
$l_8(\lambda)$	$h_8(\lambda)$	-	-	0.18413	0.07724	-	-
$l_9(\lambda)$	$h_9(\lambda)$	0.19677	0.15089	-	-	0.20259	0.19121
$l_{10}(\lambda)$	$h_{10}(\lambda)$	-	-	-	-	0.22154	0.20637

**Table 8.** Parameters  $l, h$  for the stub impedance matching configuration (III).

$V$		1001011110		0110111110		0100011100	
$l_1(\lambda)$	$h_1(\lambda)$	0.32228	0.06294	-	-	-	-
$l_2(\lambda)$	$h_2(\lambda)$	-	-	0.33396	0.07609	0.32862	0.06581
$l_3(\lambda)$	$h_3(\lambda)$	-	-	0.30586	0.09272	-	-
$l_4(\lambda)$	$h_4(\lambda)$	0.27131	0.07517	-	-	-	-
$l_5(\lambda)$	$h_5(\lambda)$	-	-	0.16840	0.10887	-	-
$l_6(\lambda)$	$h_6(\lambda)$	0.26747	0.05944	0.16656	0.08041	0.25697	0.05888
$l_7(\lambda)$	$h_7(\lambda)$	0.18786	0.05922	0.17943	0.06999	0.18086	0.05849
$l_8(\lambda)$	$h_8(\lambda)$	0.13207	0.11812	0.13723	0.12797	0.17870	0.09697
$l_9(\lambda)$	$h_9(\lambda)$	0.14578	0.19195	0.15306	0.18695	-	-
$l_{10}(\lambda)$	$h_{10}(\lambda)$	-	-	-	-	-	-

parasitic elements shown in Table 2, are realized in Figs. 5–13. One easily observes that the narrower diagrams are the ones given in Figs. 7–11. The reason is that for each of the directions nearer to the  $x$ -axis (i.e.,  $10^\circ$ ,  $30^\circ$ ,  $150^\circ$ ,  $170^\circ$ ), the symmetry results in two symmetric beams which are not clearly distinguished. In Fig. 6, for example, there are two symmetric beams at  $+28.864^\circ$  and  $-28.864^\circ$  and  $U(0)$  is only 1 dB lower than the maximum value.

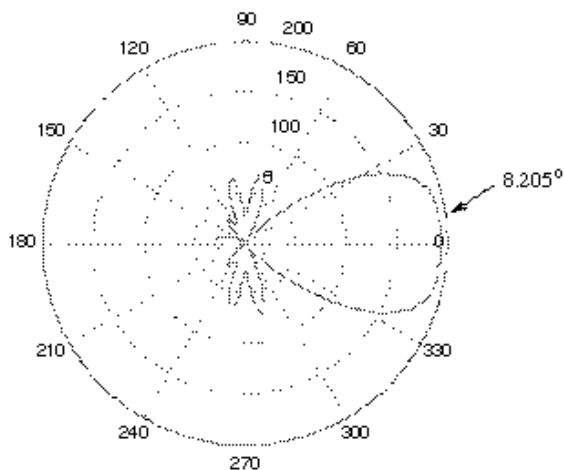


**Figure 5.** Radiation pattern for the azimuth plane of a linear array of 10 dipoles with direction of maximum gain at  $8.205^\circ$  ( $V = 1110111001$ ).

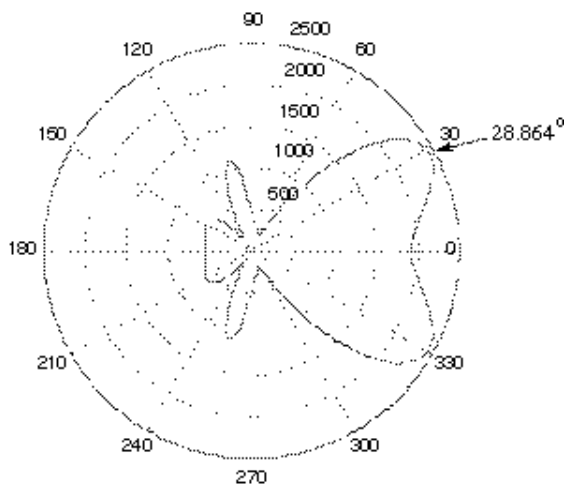


**Figure 6.** Radiation pattern for the azimuth plane of a linear array of 10 dipoles with direction of maximum gain at  $28.864^\circ$  ( $V = 0010011010$ ).

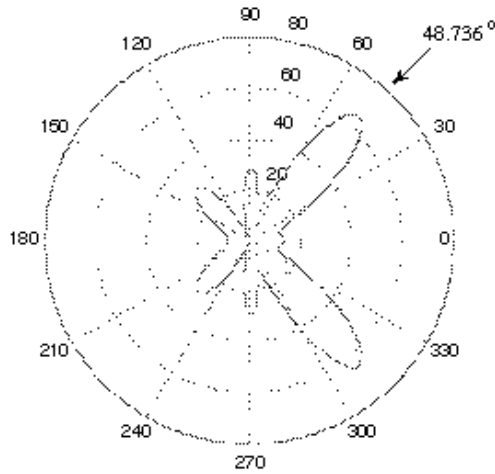


**Figure 7.** Radiation pattern for the azimuth plane of a linear array of 10 dipoles with direction of maximum gain at  $48.736^\circ$  ( $V = 1100000100$ ).

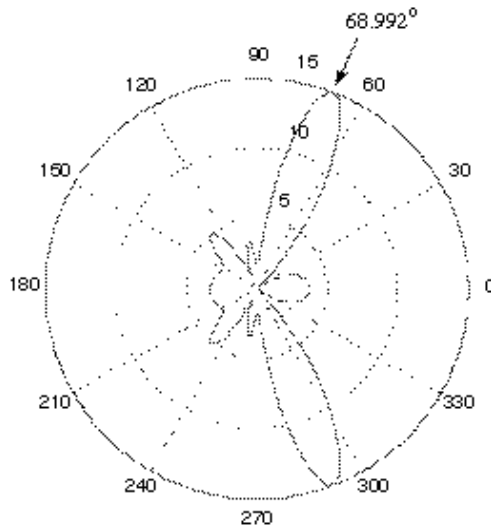


**Figure 8.** Radiation pattern for the azimuth plane of a linear array of 10 dipoles with direction of maximum gain at  $68.992^\circ$  ( $V = 1001111010$ ).

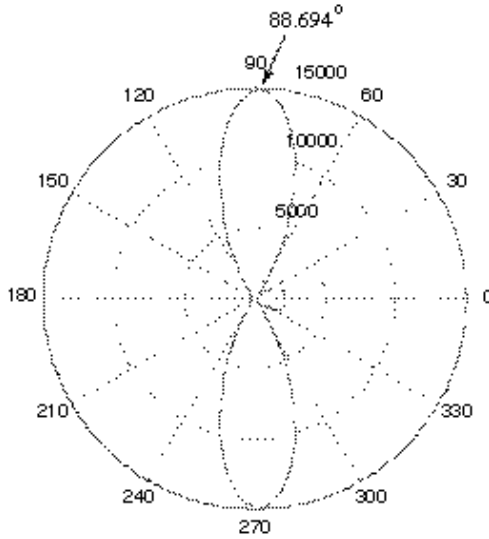


**Figure 9.** Radiation pattern for the azimuth plane of a linear array of 10 dipoles with direction of maximum gain at  $88.694^\circ$  ( $V = 0001001100$ ).

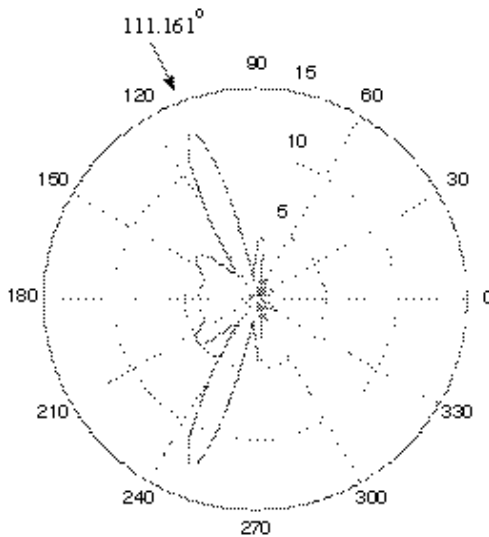


**Figure 10.** Radiation pattern for the azimuth plane of a linear array of 10 dipoles with direction of maximum gain at  $111.161^\circ$  ( $V = 0100110011$ ).

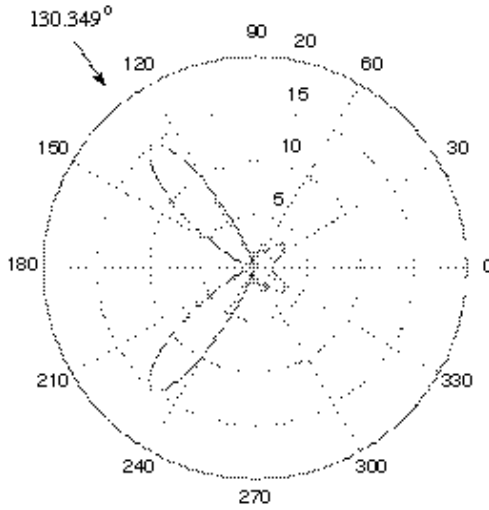


**Figure 11.** Radiation pattern for the azimuth plane of a linear array of 10 dipoles with direction of maximum gain at  $130.349^\circ$  ( $V = 1001011110$ ).

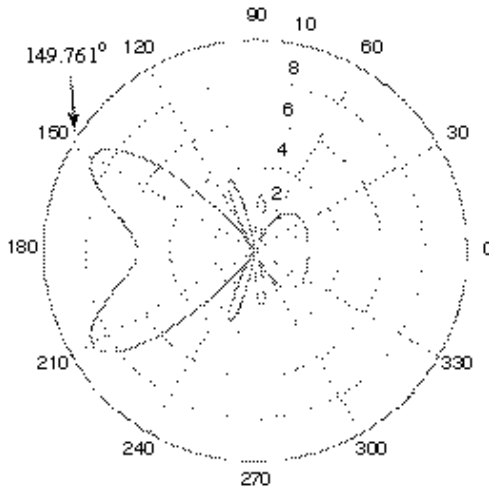


**Figure 12.** Radiation pattern for the azimuth plane of a linear array of 10 dipoles with direction of maximum gain at  $149.761^\circ$  ( $V = 0110111110$ ).



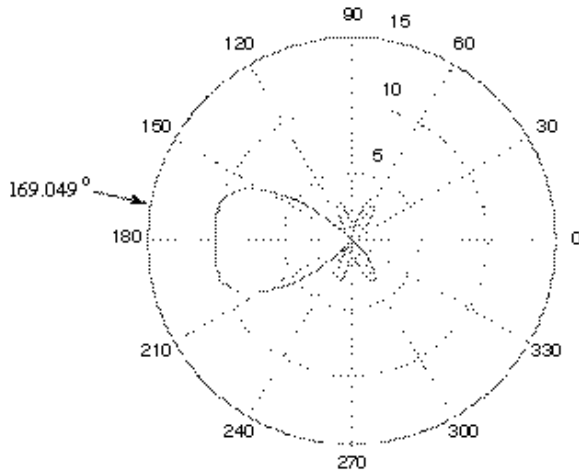


**Figure 13.** Radiation pattern for the azimuth plane of a linear array of 10 dipoles with direction of maximum gain at  $169.049^\circ$  ( $V = 0100011100$ ).

**Table 9.** Element spacing and phases for the 11-element array.

Element	Spacing ( $\lambda$ )	Phase (rad)
1	-	1.04860
2	0.31095	1.23731
3	0.39267	5.30822
4	0.34624	3.40509
5	0.20323	6.24790
6	0.48553	5.48005
7	0.12336	1.46590
8	0.30352	5.28981
9	0.14751	3.49023
10	0.78270	6.20801
11	0.23294	2.66945

**Table 10.** Directions of maximum gain, beamwidths and relative sidelobe levels.

$n$	$V$	$\varphi_{max}(^{\circ})$	$\varphi_{-}(^{\circ})$	$\varphi_{+}(^{\circ})$	$\Delta\varphi_{3dB}(^{\circ})$	R.S.L. (dB)
933	01110100101	9.082	-31.60	31.60	63.20	-3.08
719	01011001111	30.669	16.56	40.44	23.88	-3.37
921	01110011001	49.186	37.53	58.01	20.48	-7.69
249	00011111001	70.062	57.82	79.71	21.89	-3.27
48	00000110000	89.685	71.21	105.22	34.01	-6.11
343	00101010111	111.650	96.66	131.17	34.51	-4.81
315	00100111011	130.707	122.15	140.22	18.07	-4.31
183	00010110111	148.841	132.18	227.82	95.64	-3.25
1285	10100000101	168.214	151.78	208.22	56.44	-3.88

Finally, an effort was made to increase the number of elements (from 10 to 11) and compare the new solution to the previous one. This new solution (found after running a GA and following a procedure similar to the one described before) is shown in Tables 9, 10. Comparing Tables 2 and 10, one may notice that the average beamwidth using 11 elements is reduced from  $51.7^{\circ}$  to  $40.9^{\circ}$ , without decreasing of the main to secondary sidelobe ratios ( $-4.7$  dB using 10 elements and  $-4.4$  dB using 11 elements). An interesting point is that the beamwidth for  $30^{\circ}$  is impressively narrower than the one produced with the 10-element array (i.e.,  $23.88^{\circ}$  compared to  $98.64^{\circ}$ ). This means that by increasing the number of elements in the array, one can achieve narrower beamwidths and perhaps eliminate the bad effects of symmetry for the patterns with maximums at  $10^{\circ}$ ,  $30^{\circ}$ ,  $150^{\circ}$  and  $170^{\circ}$ .

## 5. CONCLUSIONS

Switched parasitic smart antenna arrays achieve electronic beam steering by choosing the appropriate combinations of active and parasitic elements. Genetic algorithms make it possible to design a ten-element linear array, which can cover the azimuth plane above the x-axis with nine radiation patterns. Each one of them points its main beam at a different direction, all between  $0^{\circ}$  and  $180^{\circ}$ . The average beamwidth is approximately  $50^{\circ}$ , much higher than the least required value of  $20^{\circ}$ . Narrower beamwidths occur by increasing the number

of elements. Relative sidelobe levels have a satisfying mean value of  $-4.5$  dB, which is slightly altered by increasing the number of elements. The problem of impedance matching at each element is solved using one stub for each time an element is active.

## REFERENCES

1. Goldberg, D. E., *Genetic Algorithms in Search, Optimization, and Machine Learning*, Addison-Wesley Publishing Company, Inc., 1989.
2. Jones, E. A. and W. T. Joines, "Design of Yagi-Uda antennas using genetic algorithms," *IEEE Transactions on Antennas and Propagation*, Vol. 45, No. 9, 1386–1392, September 1997.
3. Ares-Pena, F. J., J. A. Rodriguez-Gonzalez, E. Villanueva-Lopez, and S. R. Rengarajan, "Genetic algorithms in the design and optimization of antenna array patterns," *IEEE Transactions on Antennas and Propagation*, Vol. 47, No. 3, 506–510, March 1999.
4. Preston, S. L., D. V. Thiel, J. W. Lu, S. G. O' Keefe, and T. S. Bird, "Electronic beam steering using switched parasitic patch elements," *Electronics Letters*, Vol. 3, No. 1, 7–8, 1997.
5. Preston, S. L., D. V. Thiel, T. A. Smith, S. G. O' Keefe, and J. W. Lu, "Base-station tracking in mobile communications using a switched parasitic antenna array," *IEEE Transactions on Antennas and Propagation*, Vol. 46, No. 6, 841–844, June 1998.
6. Schlub, R., D. V. Thiel, J. W. Lu, and S. G. O' Keefe, "Dual-band six-element switched parasitic array for smart antenna cellular communications systems," *Electronics Letters*, Vol. 36, No. 16, 1342–1343, 2000.
7. Houck, C. R., J. A. Joines, and M. G. Kay, "A genetic algorithm for function optimization: A Matlab implementation," <http://www.ie.ncsu.edu:80/mirage/GAToolBox/gaot/>
8. Balanis, C. A., *Antenna Theory Analysis and Design*, 2nd Edition, John Wiley and Sons, 1997.